Hole burning and optically detected fluorine NMR in Pr^{3+}: CaF_2

D. P. Burum, R. M. Shelby, and R. M. Macfarlane
IBM Research Laboratory, 5600 Cottle Rd., San Jose, California 95193
(Received 9 October 1981)

The interactions between Pr^{3+} ions in a tetragonal site of 0.01-at. % Pr^{3+}:CaF_2 and the surrounding nuclei are investigated, primarily by means of optically detected NMR (ODNMR). This technique is based on the fact that hole burning in the 5941-Å $^3H_4 \leftrightarrow {}^1D_2$ transition takes place due to coupling between the rare-earth ion and neighboring ^{19}F nuclear spins. ODNMR lines are identified which are due to nearest-neighbor (NN), next-nearest-neighbor (NNN), and interstitial (*i*) fluorines. The distorted positions of the NNN fluorines are determined from the ODNMR data, but this is impossible for the other near neighbors due to strong covalent-bonding effects. Physical models for the hole-burning and refilling processes are proposed which agree qualitatively with the hole shapes and ODNMR line intensities, and with the observation of rf-assisted optical hole burning when a strong magnetic field H_0 is applied parallel to C_4.

I. INTRODUCTION

For rare-earth ions and other impurity systems at low temperature and concentration, magnetic interactions with host nuclei often play an important role in determining the optical dephasing time,[1] and these interactions can also provide a mechanism for optical hole burning.[2] In general, the dynamics of the near-neighbor nuclei are strongly affected by their interaction with the rare-earth ions, since this interaction is usually stronger than the homonuclear coupling in the host. The perturbed nuclei are thus detuned from the bulk, resulting in a "frozen core" of near neighbors for which the normal process of mutual spin flips has been suppressed.[3]

Pr^{3+} in a tetragonal site of CaF_2 exhibits an optical absorption at 5941 Å, corresponding to transitions between the lowest crystal-field components of $^3H_4$ and $^1D_2$.[4] We have found that this an excellent system for investigating interactions between a rare-earth ion and host nuclei. Since the electronic ground state is doubly degenerate while the excited state is a singlet,[2] the optical transition frequency is sensitive to magnetic fields, so that the surrounding fluorine ions have a strong effect on the optical dephasing time. Furthermore, when the praseodymium is in its ground state, spin flips of near-neighbor fluorines are inhibited due to the strong detuning effect of the electronic magnetic moment, giving rise to a large frozen core of ^{19}F nuclei. As was reported recently,[2] nuclear spin flips within the frozen core provide the dominant mechanism for hole burning in this site.

An unusual feature of this site is the fact that for dopant concentrations less than 0.1 at. %, hyperfine lines with splittings of 2.77 GHz, are clearly resolved.[2] An example is shown in Fig. 1. When a hole was burned in one hyperfine line, antiholes appeared immediately adjacent to the hole which agreed closely in shape with the predictions of a model based on optically induced, frozen-core fluorine spin flips, as shown in Fig. 2.

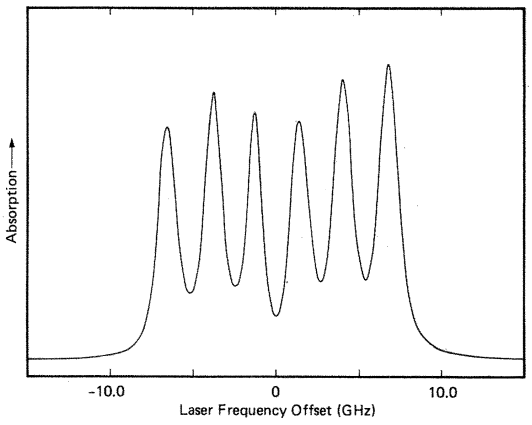

FIG. 1. Fluorescence excitation spectrum of the $^1D_2 \leftrightarrow {}^3H_4$ transition (5941 Å) in the tetragonal site of 0.01-at. % Pr^{3+}:CaF_2 at 1.6 K.

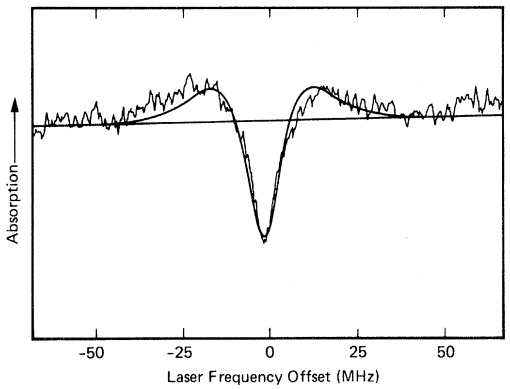

FIG. 2. Excitation spectrum of a hole burned in one of the hyperfine lines of 0.01-at. % Pr^{3+}:CaF_2. The width of the hole (FWHM) is 9 MHz and antiholes due to near-neighbor fluorines separated by ~ 10 MHz from the hole are clearly visible. The solid curve is based on a theoretical model involving spin flips of the near-neighbor fluorines while the Pr^{3+} ion is in its ground state.

The most direct verification of this hole-burning mechanism was the demonstration that rf irradiation in resonance with one or more of the near-neighbor fluorine spins could be used to fill in an optical hole.[2] This, in turn, provides a technique[5] by which the nuclear magnetic resonances of individual fluorines in the frozen core can be optically detected (ODNMR). We have used this technique to determine the directions and magnitudes of the local Pr^{3+} magnetic fields at the nearest-neighbor and next-nearest-neighbor fluorine sites, and this has enabled us to make inferences concerning the distortion of the lattice due to the insertion of the rare-earth ion.[6]

In the next two sections our general spectroscopic results on the tetragonal site in Pr^{3+}:CaF_2 are given, and a basic physical model for the hole-burning ODNMR experiment is briefly discussed. Then, after some experimental details, our ODNMR results are presented. Finally, some discussion and conclusions are contained in the last section.

II. SPECTROSCOPY OF THE 5941-Å TETRAGONAL SITE

The crystal structure of CaF_2 consists of a simple cubic lattice of F^- ions with a Ca^{2+} ion at the body center of every other cube.[7] In the site studied, the Pr^{3+} ion replaces a Ca^{2+} ion and an extra, interstitial fluorine is included in one of the neighboring vacant body centers for charge compensation, resulting in a site with C_{4v} symmetry.[8] The 5941-Å absorption line was originally identified as corresponding to a tetragonal site by Evesque *et al.*[4] The optical and ODNMR measurements reported here provide unequivocal confirmation of this assignment as well as the nature of charge compensation for this site.

Selective excitation and emission spectra of this site showed an additional absorption line at 5935 Å and three broad emissions at 6098, 6136, and 6141 Å. Thus $^1D_2$ levels are observed at 16 830 and 16 850 cm^{-1} and $^3H_4$ levels at 0, 430, 535, and 550 cm^{-1}. No evidence of energy transfer between this site and any of the others present was observed at the concentrations studied.

A high-resolution (~ 1 MHz) absorption spectrum of the 5941-Å line was recorded with a cw dye laser (using fluorescence excitation) and is shown in Fig. 1. The spectrum exhibits clearly resolved hyperfine structure consisting of six hyperfine lines. The splittings are all equal to 2770 MHz except for the center splitting, which is 2870 MHz. This results in the deeper minimum between the center two lines (Fig. 1), which indicates a residual splitting of the non-Kramers doublet by nontetragonal strain fields that increase the center splitting and decrease the others. No linear variation of splittings due to second-order hyperfine coupling in ground or excited states was observed.

The inhomogeneous linewidths [full width at half maximum (FWHM)] are 650 MHz at 0.001-at. % Pr^{3+} (Ref. 2) and 1.26 GHz at 0.01 wt. %, and they increase rapidly with increasing dopant level. By absorption and fluorescence measurements in a high magnetic field it was determined that the ground state is doubly degenerate, with $g_{||}\beta/h = 5.5$ MHz/G and $g_{\perp}\beta/h = 0$, where the orientation is with respect to the C_4 axis. The transition is allowed for light polarized perpendicular to the C_4 axis. From the selection rules for C_{4v} symmetry, this shows that the excited state is electronically nondegenerate. With the laser-beam-propagation axis aligned along the [100] axis it is possible to avoid exciting either the group of Pr^{3+} ions with the C_4 axis along the [010] axis or the group with C_4 along the [001] axis by polarizing the laser along [010] or [001], respectively. Application of a magnetic field along the [010] axis splits the optical hyperfine lines for which C_4 is parallel to the magnetic field away from the lines

for which C_4 is perpendicular to the field. With an applied field perpendicular to the laser beam it then is possible to irradiate only a single set of Pr^{3+} ions with C_4 either along the laser beam or along the field by either selecting the unsplit hyperfine lines and polarizing the laser parallel to the field, or selecting the split lines and polarizing the laser perpendicular to the field. This selectivity was helpful in assigning the ODNMR lines which were observed, as discussed below.

The ground-state hyperfine structure is very close to that inferred from ultrasonic paramagnetic-resonance measurements of (presumably) the same tetragonal center,[9] i.e., $A_{||}=2770$ MHz and $g_{||}=1.94$ (5.45 MHz/G), for an effective spin of 1. For a level with E symmetry derived from a T_2 level in cubic symmetry one predicts $A_{||}=2733$ MHz and $g_{||}=2$. This agreement indicates that very little mixing has taken place with the other E level arising from the $J=4$ ground state. A nearby level of B_2 symmetry should also be present, but is not observed in the emission spectrum due to selection rules.

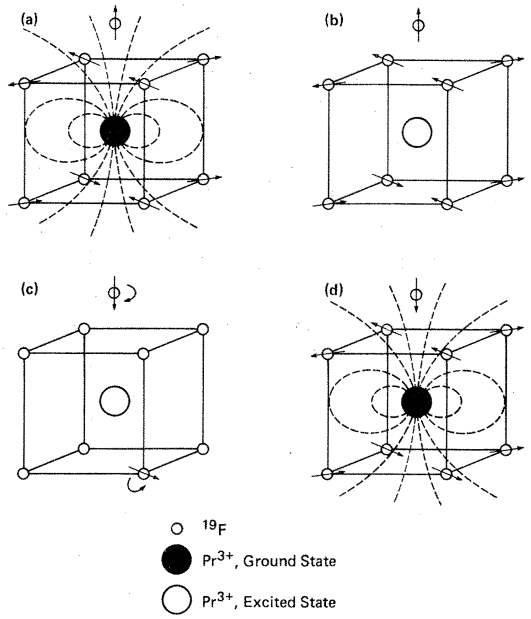

FIG. 3. Pictorial representation of the physical model for hole burning in the site studied. (a) While the praseodymium ion is in its ground state, spin flips of the surrounding fluorines are inhibited due to strong coupling with the Pr^{3+} magnetic field. (b) When the Pr^{3+} is optically excited its magnetic field all but vanishes, leaving the near-neighbor fluorine nuclei more or less free to undergo spin flips. (c) The praseodymium typically remains excited long enough for several near-neighbor fluorine spin flips to occur. In the figure, spin flips of the interstitial and one of the nearest neighbors have been indicated as representative examples. (d) Finally, when the Pr^{3+} ion returns to its ground state it is no longer in resonance with the laser, due to the energy shift caused by the near-neighbor fluorine nuclear-spin flips. Note that only the nearest-neighbor fluorines and the interstitial are included in this figure, although ODNMR measurements have established that spin flips of the next-nearest neighbors also contribute to the hole-burning process.

III. PHYSICAL MODEL OF THE HOLE-BURNING PROCESS

The basic hole-burning mechanism is depicted in Fig. 3. When the Pr^{3+} ion is in the ground state [Fig. 3(a)] the near neighbors are strongly detuned from one another and from the bulk due to their coupling with the praseodymium electron moment. The result is a frozen core of near neighbors, as mentioned earlier, in which mutual fluorine spin flips are suppressed. When the praseodymium electron is optically excited to a singly degenerate state [Fig. 3(b)], the Pr^{3+} magnetic moment is reduced by roughly 3 orders of magnitude, and as illustrated in Fig. 3(c) the spin-flip rates of the surrounding fluorines become faster than the excited-state lifetime of 509 μsec. Finally, when the praseodymium ion returns to its ground state [Fig. 3(d)] its energy is shifted out of resonance with the laser due to the changes in the nuclear-spin states of the surrounding fluorines. According to the ODNMR frequencies reported in the next section, this shift in optical frequency is typically 20—30 MHz.

The hole-burning process is illustrated in terms of energy levels in Fig. 4. Since the Pr^{3+} site has axial symmetry, the z component of the praseodymium nuclear spin is a good quantum number, and there is only one allowed optical transition from a given ground-state hyperfine level. However, each hyperfine level is split into a number of superhyperfine levels through the magnetic coupling between the rare-earth ion and the surrounding fluorine atoms. Spin flips of these fluorines while the system is in its optically excited state result in depletion of the superhyperfine level which is irradiated by the laser.

As shown in Fig. 2, the hole-burning spectrum for Pr^{3+}:CaF_2 consists of only a single, broad line without any resolved superhyperfine structure. The hole width of 9 MHz (FWHM) is much greater than both the 430-kHz homogeneous

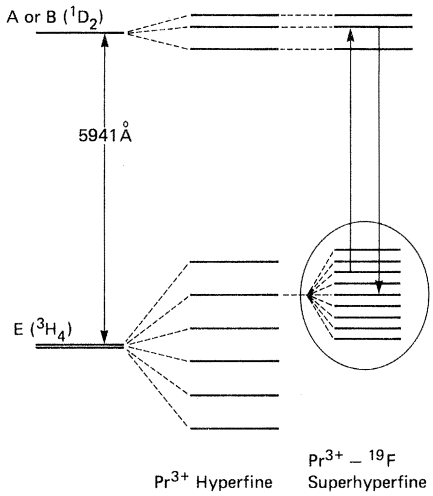

FIG. 4. Energy-level diagram illustrating the hole-burning mechanism in the site studied. The effect of the Pr^{3+} hyperfine interaction on the doubly degenerate $^3H_4$ ground state and the nondegenerate $^1D_2$ excited state at 5941 Å is indicated. Superhyperfine interactions with the surrounding fluorine nuclei further split each of the six ground-state hyperfine levels while the excited-state levels remain virtually unaffected. For simplicity, the splitting of just one of the hyperfine lines due to only its eight nearest neighbors has been indicated in the magnified (circled) region on the right-hand side of the figure. Owing to fluorine spin flips while the Pr^{3+} is in its excited state, the system may return to a different ground-state superhyperfine level after an optical pumping cycle, as indicated in the figure. This shifts the system out of resonance with the laser, resulting in hole burning.

linewidth which we measured from optical free-induction decay, and the contributions expected from power-broadening and laser-frequency jitter. Instead, the width is caused by slow spectral diffusion within the frozen core of fluorine nuclei. The validity of this explanation is supported by the close agreement which can be seen in Fig. 2 between the experimental data and the solid curve based on a theoretical model. This model assumes that there is a large number of identical near-neighbor fluorines undergoing random spin flips which shift the optical resonance frequency of the system. Other than adjustment of the horizontal and vertical scales and Gaussian broadening, the model involves only one adjustable parameter, namely the average fraction of fluorine spins which flip during an optical pumping cycle while the Pr^{3+} ion is in its excited state.

If rf irradiation is applied to the sample with a frequency resonant with one or more near-neighbor fluorines, the frozen-core spin-flip rate is artificially increased and the hole becomes shallower. Signals of up to 40% hole filling were observed in some cases. One example appears in Fig. 5, which shows the change in fluorescence due to application of resonant, square-wave-gated rf. The effect of the rf on the frozen-core flip rate is apparent not only from the changes in the equilibrium fluorescence level (corresponding to changes in the hole depth) but also from the fact that the system approaches equilibrium much more rapidly during rf irradiation than it does after the rf is turned off.

IV. EXPERIMENTAL

A crystal of 0.01-at. % Pr^{3+}:CaF_2 of roughly cylindrical shape with a length of $\simeq$ 5 mm and a diameter of $\simeq$1.5 mm was oriented such that the laser beam and the applied external field lay along two of the three orthogonal (100) crystal axes. Since $g_\perp = 0$, the crystal was aligned by minimizing the splitting at $H_0 = 15$ kG of the optical lines for which $\vec{H}_0 \perp \vec{C}_4$. Owing to the narrow inhomogeneous linewidth of $\sim$ 1 GHz, this procedure was sufficiently sensitive to determine that misalignment was less 0.2°.

The sample was immersed in liquid He at 1.5 K,

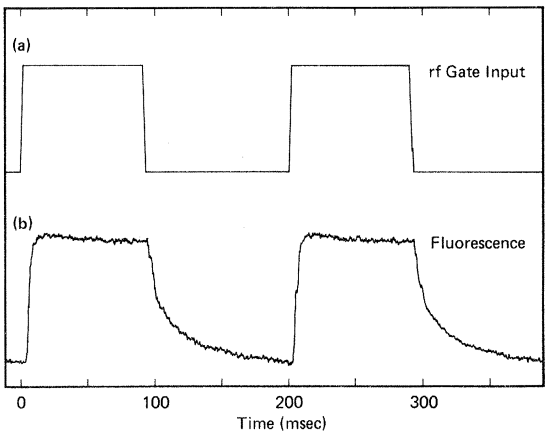

FIG. 5. The result of applying $\sim$ 5 G of square-wave-gated rf at 9.2 MHz in resonance with the four nearest-neighbor fluorines furthest from the interstitial. (a) The dc input to the rf gate. (b) Increase in fluorescence due to partial filling of the hole by the rf. Note that the increased fluorine spin-flip rate due to the rf causes the system to reach equilibrium much more quickly when the rf is switched on than when it is switched off.

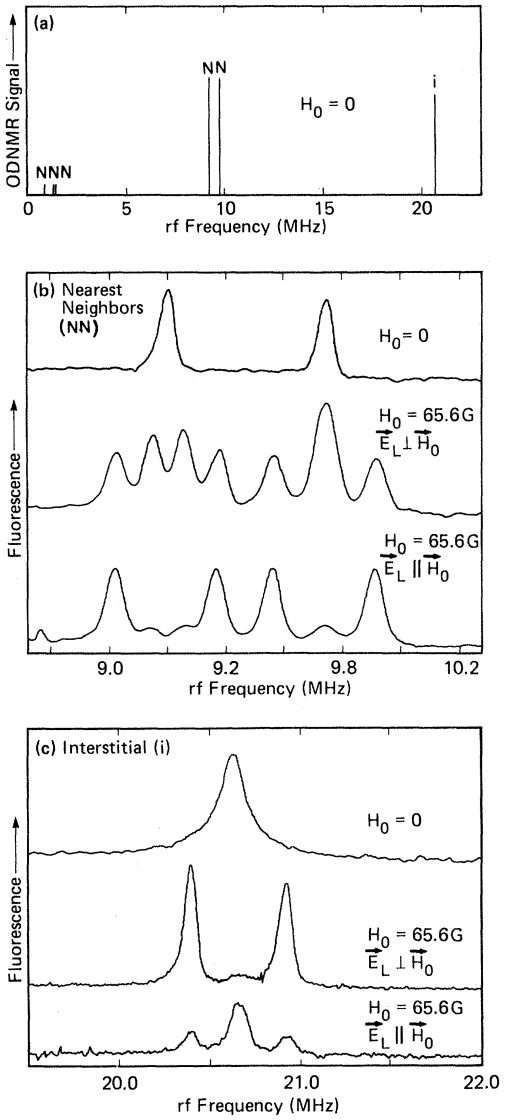

FIG. 6. ODNMR lines for the site studied, and their behavior in a small applied magnetic field. (a) Stick diagram showing the resonant frequencies and indicating the relative intensities of the six ODNMR lines with no applied external field. The assignments of the lines as nearest neighbors (NN), next-nearest neighbors (NNN), and the interstitial fluorine (*i*) are indicated. (b) Splittings of the two NN lines near 10 MHz in an applied field. At higher fields both multiplets became quartets. (c) Splitting of the interstitial ODNMR line near 20 MHz in a field. This multiplet remained a triplet at all field strengths. The amplitude of the bottom trace has been multiplied by 2 relative to the other two traces near 20 MHz. Note that rotating the laser polarization from $\vec{E}_L \perp \vec{H}_0$ to $\vec{E}_L \| \vec{H}_0$, which eliminates the signal corresponding to $C_4 \| \vec{H}_0$, suppressed the inner lines in part (b) but tended to suppress the outer lines relative to the inner line in part (c).

and was surrounded by an rf coil of traveling-wave design[10] with approximately flat response for rf frequencies between 0.5 and 100 MHz. The axis of the coil was coincident with the laser beam and with the cylinder axis of the sample. A superconducting magnet supplied the static field H_0, for which the inhomogeneity over the sample volume was less than the bulk fluorine dipolar width in CaF_2 of about 10 kHz.

A cw single-frequency dye laser with a jitter width of $\simeq$ 1 MHz was used to irradiate the sample with about 40 mW of light in a $\sim$1-mm diameter beam. For the ODNMR measurements the laser frequency was tuned to a specific hyperfine line and the sample fluorescence was monitored while an rf field of about 0.01$-$0.1 G was applied to the sample. The spectra were obtained by square-wave gating the rf at 5 Hz and feeding the fluorescence signal into a lock-in amplifier, the output of which was plotted directly on an *X-Y* recorder as the rf frequency was swept.

V. RESULTS

At zero applied magnetic field, six ODNMR lines were observed at 0.87, 1.34, 1.40, 9.20, 9.75, and 20.65 MHz. The three lines near 1 MHz were much weaker than the others, as indicated schematically in Fig. 6(a). When a small magnetic field was applied along a [100] axis perpendicular to the laser beam, the three strong lines split into multiplets, as shown in Fig. 6(b) and 6(c). Several observations enabled us to assign these multiplets to near-neighbor fluorines. First, at stronger applied fields with the laser polarized such that the electric vector $\vec{E}_L$ is perpendicular to H_0 both of the multiplets shown in Fig. 6(b) became quartets whereas the multiplet in Fig. 6(c) remained a triplet. Second, as shown in the figure, rotating the laser polarization from $\vec{E}_L \perp \vec{H}_0$ to $\vec{E}_L \| \vec{H}_0$, suppressed the inner lines of the multiplets near 10 MHz and the outer lines of the multiplet near 20 MHz. This implies that the local praseodymium field is roughly perpendicular to the C_4 axis for the 10-MHz multiplets, and parallel to C_4 for the 20-MHz multiplet. Finally, the splitting of the outer lines in Fig. 6(c) is $2\gamma_f H_0$, to within our ability to independently determine H_0, where $2\pi\gamma_f = 4$kHz/G is the fluorine gyromagnetic ratio, while the outer splittings in Fig. 6(b) are roughly $\sqrt{2}\gamma_f H_0$.

The assignment of the resonance lines indicated in Fig. 6(a) was made as follows. In the absence of

lattice distortions, the nearest-neighbor (NN) fluorines are located on the corners of a cube surrounding the Pr^{3+} ion. Thus, if one assumes that the Pr^{3+} magnetic field is point dipolar in nature, the local fields at the nearest-neighbor fluorine sites will be nearly perpendicular to the C_4 [100] axis and will make an angle of nearly $\pi/4$ with the [010] and [001] axes. Setting the laser polarization parallel to the applied field will select out only those sites for which $H_0 \perp C_4$, so that the only observable ODNMR lines due to nearest-neighbor fluorines will be those with splittings near $\sqrt{2}\gamma_f H_0$, and the nearest-neighbor fluorine lines with $C_4 \| H_0$, on which H_0 has only a small effect, will be suppressed. Clearly, both the measured splitting values and the behavior with laser polarization indicate that the two ODNMR multiplets near 10 MHz are due to the nearest-neighbor fluorines.

Even if no assumptions are made regarding the nature of the Pr^{3+} magnetic field or the lattice distortions, symmetry requires the local field at the site of the interstitial fluorine to be parallel to the C_4 axis. Because of this, the splitting of the ODNMR lines for H_0 parallel to C_4 will be exactly equal to $2\gamma_f H_0$, and these lines will be suppressed when the laser polarization is parallel to H_0 leaving only a single line corresponding to $H_0 \perp C_4$. Therefore, comparison with Fig. 6(c) indicates that the multiplet near 20 MHz is due to the interstitial fluorine.

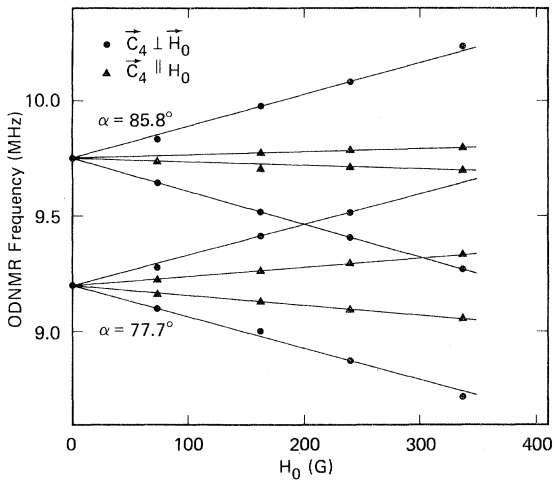

FIG. 7. ODNMR line positions for the two nearest-neighbor multiplets near 10 MHz as a function of applied field. From these splitting curves the values indicated in the figure for the angle α between the local Pr^{3+}-field direction at the fluorine site and the C_4 axis were determined. The splitting curves for the ODNMR multiplet centered at 20.65 MHz, for which symmetry demands that $\alpha=0$, were used to calibrate the magnetic field.

The splitting of the outer two lines in the interstitial fluorine multiplet centered at about 20.65 MHz was used as an accurate calibration of the applied field strength, and the splittings of the two multiplets near 10 MHz were measured as a function of H_0. The results are shown in Fig. 7.

Since the external field adds vectorially to the local field due to the Pr^{3+} ion at the fluorine site, the splittings of the ODNMR lines in a small field can be used to calculate the angle α between the C_4 axis and the local field. Because symmetry requires the azimuthal angle to be zero, this determines the local praseodymium field direction. Unfortunately, the dependence of α on the position of the fluorine is difficult to determine in general, due to covalent-bonding effects.[8] However, for the more-distant neighbors the Pr^{3+} magnetic field can be assumed to be essentially point dipolar. This allows the distance between the two nuclei and the angle θ between the internuclear vector and the C_4 axis to be calculated. By symmetry, this determines the position of the fluorine.

In principle, the splitting curves for either $C_4 \perp \vec{H}_0$ or $C_4 \| \vec{H}_0$ in Fig. 7 can be used to determine α for the two groups of equivalent nearest-neighbor fluorines. The $C_4 \perp H_0$ data are more sensitive to α, and were used to obtain the values $\alpha = 77.7° \pm 0.5°$ for the multiplet centered at 9.2 MHz and $\alpha = 85.8° \pm 0.5°$ for the multiplet centered at 9.75 MHz. As a check, these values of α were used to calculate theoretical splitting factors for $C_4 \| H_0$ for the two multiplets. The calculated values of 0.69 $(2\gamma_f)$ and 0.71 $(2\gamma_f)$ compare favorably with the measured values of 0.66 $(2\gamma_f)$ and $0.71(2\gamma_f)$. The factors of 2 in the splittings arise because the applied field adds to one set of nuclei and subtracts from another. Thus, the multiplets are actually groups of symmetrically shifted ODNMR lines, and not really "split" lines in the usual NMR sense.

Since the value of α for the multiplet centered at 9.2 MHz was closest to the value $\alpha = 90°$ corresponding to a purely dipolar field and an undistorted lattice, this multiplet was tentatively assigned to the group of four nearest-neighbor fluorines which are furthest from the interstitial.

It should be clear from the assignments already made that the three ODNMR lines observed at zero applied field near 1 MHz are due to next-

TABLE I. Next-nearest-neighbor fluorine positions as obtained from low-field ODNMR data.

Measured data Frequencies (MHz)		Theoretical fit Frequencies (MHz)					
$H_0=0$	$H_0=35.4$ G	$H_0=0$	$H_0=35.4$ G	α	r^a	θ	^{19}F Positions[a]
	0.78		0.78				
0.87		0.87		46.2°	0.815a	73.9°	$(\pm0.78,\pm0.45,\pm0.45)a$ $(\pm0.45,\pm0.78,\pm0.45)a$
	0.98		0.97				
	1.23		1.22				
1.34		1.34		33.1°	0.842a	21.8°	$(\pm0.43,\pm0.43,+0.78)a$
	1.47		1.46				
	1.30		1.27[b]				
1.40		1.38[b]		39.0°[b]	0.829a[b]	25.2°[b]	$(\pm0.5,\pm0.5,-0.75)a$[b]
	1.52		1.49[b]				

[a]The lattice constant $a=5.46$ Å.
[b]Value calculated for no lattice distortion and no covalent-bonding effects.

nearest-neighbor fluorines. This assignment is strengthened by the fact that the measured resonance frequencies are very close to the values calculated under the assumption of only point dipolar interactions and no lattice distortion, as shown in Table I. Unfortunately, it was not possible to obtain splitting factor curves such as those shown in Fig. 7 for these three ODNMR lines, since they rapidly became unobservable when an external field was applied. However, by utilizing a signal-enhancement technique it was possible to make a single splitting measurement at very low applied field. It was found that simultaneous, cw rf irradiation of one or more of the strong ODNMR lines at zero field dramatically enhanced the amplitudes of the 1-MHz lines with zero applied field, as illustrated in Fig. 8. Apparently, saturation of the nearest-neighbor and interstitial ODNMR lines with rf prevents these fluorines from participating in the hole-burning process, and therefore greatly increases the number of rare-earth ions which participate in the hole burning via spin flips of next-nearest neighbors.

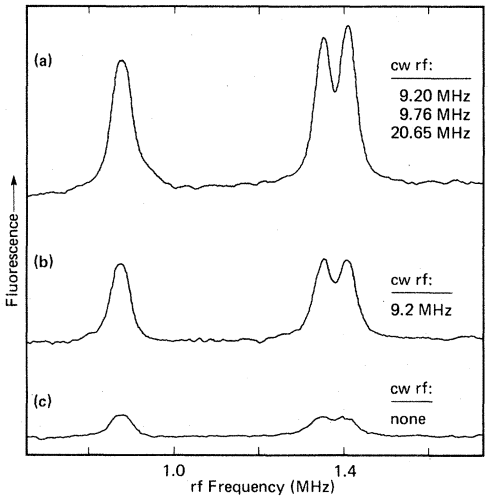

FIG. 8. Enhancement of the next-nearest-neighbor fluorine ODNMR lines via cw rf saturation of the nearest neighbor and interstitial lines. (a) Maximum enhancement, attained by saturating all three strong ODNMR lines. (b) Enhancement when only the nearest-neighbor ODNMR line at 9.2 MHz was irradiated. (c) The unenhanced next-nearest-neighbor spectrum.

By applying cw rf irradiation to one member of each of the three strong multiplets with $\vec{E}_L \| \vec{H}_0$, it was possible to obtain splittings at $H_0=35.4$ G for the three lines near 1 MHz. From this measurement, values of α were obtained for the three lines, and these were used along with the zero-field resonance frequencies to calculate the positions of the next-nearest-neighbor fluorines under the point dipolar field assumption. The results are presented in Table I. The calculated next-nearest-neighbor positions given in the table are all very close to the undistorted lattice positions, which makes the assignment of these lines very simple. The only ambiguity is which of the two NNN lines near 1.4 MHz is due to the four next-nearest neighbors closest to the interstitial and which is due to the set of four which are furthest from the interstitial. Since the fluorine positions calculated from the line with a frequency of 1.40 MHz at $H_0=0$ are indistinguishable from the undistorted case within

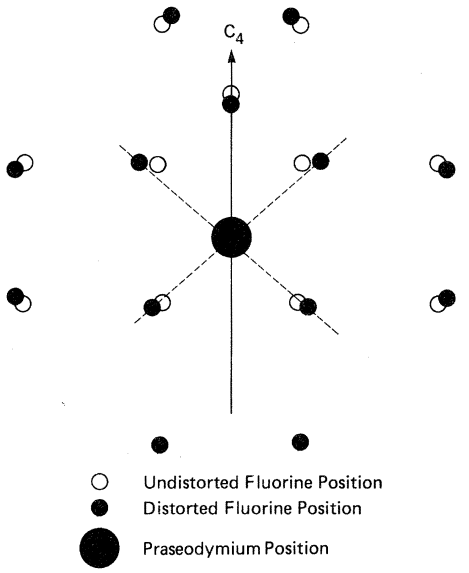

FIG. 9. Projection of the normal and distorted fluorine and Pr^{3+} positions on a plane containing the C_4 symmetry axis and one of the other [100] axes. The projections of eight of the next-nearest neighbors, which would have overlapped with those of the nearest neighbors, have been omitted. The distorted next-nearest-neighbor positions indicated were determined from their measured local Pr^{3+} fields. The distorted nearest-neighbor positions were then chosen on the basis of these NNN positions. The dashed lines in the figure indicate the axes along which the nearest neighbors must lie if the covalent-bonding effects are assumed to be entirely point dipolar in form.

experimental error, this line was tentatively assigned to the group of four next-nearest neighbors furthest from the interstitial. It then follows that the line at 1.34 MHz corresponds to the next-nearest neighbors which are closest to the interstitial, and of course the line at 0.87 MHz is due to the 16 next-nearest neighbors which are in between. The distorted positions of the next-nearest neighbors are illustrated in Fig. 9, which compares them with their undistorted positions.

As a check on our understanding of the low-field data, ODNMR measurements were also made at $H_0 \simeq 16.6$ kG. At this high external field strength only the parallel component of the Pr^{3+} magnetic field is felt, and the fact that the dependence of the ODNMR frequency on applied field in this region was just the fluorine gyromagnetic ratio $2\pi\gamma_f = 4$ kHz/G served to further verify that the hole burning and ODNMR effects are due to neighboring fluorine spins. As can be seen from Table II, all of the frequencies of the ODNMR lines which were detected agree closely with the values predicted from the low-field data.

With one exception, namely the interstitial fluorine lines for $C_4 \| \vec{H}_0$, all of the ODNMR lines at high field were very weak, requiring the use of higher rf power levels which led to broadening of the resonance lines. In the cases where the applied field and the Pr^{3+} field were nearly perpendicular, i.e., the nearest-neighbor lines with $C_4 \| \vec{H}_0$ and the interstitial lines for $C_4 \perp \vec{H}_0$, the resonance signal was too weak to be detected at all. These observations are discussed in the next section.

Another interesting feature of the high-field data is shown in Fig. 10. Superimposed on a power-broadened set of next-nearest-neighbor lines for $\vec{E}_L \perp \vec{H}_0$ is a very sharp ($\sim$ 10 kHz FWHM) resonance with inverted phase which occurred at exactly the bulk fluorine resonance frequency. This phenomenon was interpreted as being rf-assisted hole burning, whereby the rf provides an extra mechanism by which the near-neighbor fluorines can undergo spin flips while the Pr^{3+} is in the excited state.

VI. DISCUSSION

A. Perturbed fluorine geometry

Tentative positions for the next-nearest-neighbor fluorines calculated under the point dipolar assumption are given in Table I. These positions are indicated in Fig. 9, which shows the projections of the praseodymium and fluorine positions on a (100) plane with the C_4 axis contained vertically in the plane. As the figure shows, all of the next-nearest neighbors are pushed away from the praseodymium but toward each other, except for the four which are furthest from the interstitial and are not displaced from their undistorted positions. Positions of the nearest-neighbor fluorines and the interstitial which were estimated from the next-nearest-neighbor positions have also been indicated in the figure. The dashed lines in Fig. 9 are the axes determined from the measured values of α along which the nearest-neighbor fluorines must lie if their coupling to the Pr^{3+} ion is assumed to be purely point dipolar in nature.

One would expect that the lattice distortions due to the substitution of a Pr^{3+} for a Ca^{2+} ion and the insertion of an interstitial fluorine would tend to displace the nearest-neighbor fluorines away from the praseodymium ion, and as Fig. 9 indicates, this expectation is supported by the displace-

TABLE II. Comparison of high-field ODNMR frequencies for NN and NNN ^{19}F nuclei with the frequencies predicted from low-field data.

H_0 (kG)	Measured Frequency (MHz ± 0.05)	Frequency predicted from low-field data (MHz)
$C_{4v}\|\|\vec{H}_0$		
16.58[a]	45.92	45.68 *i*
	—	64.96 NN
	65.68	65.70 NNN
	67.33	67.39 NNN 67.42 NNN
16.59[a]	—	67.71 NN
	87.06	87.02 *i*
$C_{4v}\perp\vec{H}_0$		
16.57[b]	59.875	59.81 NN
	60.315	60.30 NN
	65.68	65.50 NNN 65.52 NNN 65.69 NNN
	66.17	66.12 NNN
	66.42	66.46 NNN
	66.84	66.89 NNN 67.06 NNN 67.08 NNN
	—	69.43 *i*
	72.915	72.95 NN
	73.475	73.49 NN

[a]Determined from the frequency of the rf-assisted hole-burning signal.
[b]Taken from the center of symmetry of the NNN ODNMR lines.

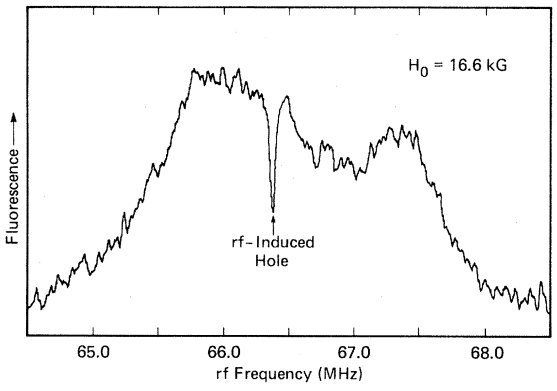

FIG. 10. ODNMR spectrum showing rf-assisted optical hole burning in the site studied for $C_4||\vec{H}_0$ at high field. The width of the dip in the fluorescence corresponding to this phenomenon, which overlaps a severely power-broadened group of unresolved NNN ODNMR lines, is only $\simeq$ 10 kHz (FWHM), corresponding to the bulk dipolar fluorine NMR linewidth. When the rf sweep rate was slowed sufficiently, the fluorescence level at the center of the dip fell nearly to the baseline.

ments of the next-nearest neighbors. Therefore, the fact that the zero-field ODNMR frequencies for the nearest neighbors are 9.2 and 9.75 MHz, as compared to the value 7.37 MHz calculated for a point-dipolar interaction in an undistorted lattice and using the praseodymium $g_{||}$ value of 5.5 MHz/G, is convincing evidence that there is a strong covalent-bonding effect. The same is even more true for the interstitial fluorine, which has a zero-field resonance frequency of 20.65 MHz instead of the point-dipole calculated value of 6.76 MHz. Note that the relative strengths of the covalent-bonding effects roughly follow the degree to which each of the surrounding fluorines plays a part in the charge compensation of the Pr^{3+} ion, since the interstitial compensates a full electronic charge, or four times as much as each of the nearest-neighbor fluorines.

In view of the strength of the covalent-bonding effects, it is suprising that the values of α obtained for the nearest-neighbor fluorines from the low-field data, $\alpha = 77.7°$ and $\alpha = 85.8°$, are so close to

the point-dipole undistorted lattice value of $\alpha = 90°$. Apparently, the additional coupling between the Pr^{3+} ion and the nearest-neighbor fluorines due to covalent-bonding effects is mostly point dipolar in form, so that the magnitudes of the effective local fields at the fluorine sites are enhanced without large changes in their directions.

B. ODNMR intensities

The fact that the ODNMR lines tend to become weaker when an external magnetic field is applied, and that this effect is strongest when the applied field is perpendicular to the local Pr^{3+} field, suggests the following mechanism. Based on the fact that typical helium-temperature, electron spin-lattice relaxation times in non-Kramers doublet systems of this type are on the order of 5 msec,[11] it can be assumed that the Pr^{3+} electron is undergoing spin flips which are rapid on the time scale of the hole-burning process. With no applied external field a spin flip of the Pr^{3+} electron will cause the sign, but not the direction, of the local field at each of the near-neighbor fluorine sites to change. Thus, the quantization axis for each fluorine in the frozen core will remain time independent. However, if there is an applied magnetic field the total local field at each nuclear site will toggle between two positions which in general will be along different quantization axes. This process will induce spin flips of the frozen-core fluorines at a rate proportional to the electron-flip rate and the sine of the angle between the applied field and the local Pr^{3+} field. These increased frozen-core spin-flip rates will lead in turn to less hole depth and weaker ODNMR lines.

The above mechanism corresponds qualitatively with the observed dependence of the ODNMR line strengths on the applied field. For small applied fields only the next-nearest-neighbor lines were strongly affected, because only for these sites was the Pr^{3+} local field small enough to be significantly perturbed by an applied field of only $\simeq 35$ G. In fact, it is possible that even at zero applied external field, the local field due to neighboring fluorines combines with the Pr^{3+}-electron spin flips to induce flips of the next-nearest-neighbor fluorines. This would explain why the next-nearest-neighbor lines are so much weaker than the other ODNMR lines at zero field.

At high external field, all the ODNMR lines were very weak except for the one case where the Pr^{3+} field and the external field were parallel, namely the interstitial fluorine with $C_4 \| \vec{H}_0$. It was also noticed that the equilibrium hole depth for $C_4 \| \vec{H}_0$, while less than at zero field, was much greater than for $C_4 \perp \vec{H}_0$. This suggests that at high field and with $C_4 \| \vec{H}_0$ the interstitial fluorine is responsible for most of the hole burning. The explanation as to why the rf-assisted hole-burning effect appeared only in this case now also becomes more apparent, since the vectors joining the interstitial fluorine with its eight nearest-neighbor fluorines are at the "magic angle" with respect to the C_4 axis, and thus, in this case, with respect to the applied field. The applied magnetic field therefore suppresses the homonuclear-dipolar interaction between the interstitial fluorine and its nearest neighbors, so that the spin-flip rate of the interstitial is slow even when the Pr^{3+} ion is in the excited state. The applied rf compensates for this effect, and so enhances the hole burning. In all other cases the fluorine spin-flip rate when the Pr^{3+} ion is optically excited is apparently great enough to preclude enhancement of the hole burning by rf.

The reappearance of next-nearest-neighbor fluorine ODNMR lines at high field (Table II) also supports the electron spin-flip mechanism suggested above. This is because the Pr^{3+} local field is too weak at these sites to tilt the total field direction very far away from the external field direction, while the much stronger local Pr^{3+} fields at the nearest-neighbor and interstitial fluorine sites are still able to have a significant effect.

VIII. CONCLUSIONS

The spectroscopy of the 5941-Å $^3H_4 \leftrightarrow {}^1D_2$ transition corresponding to a tetragonal site in 0.01 at.% Pr^{3+}: CaF_2 has been explored. As reported earlier,[2] the six ground-state hyperfine lines in the absorption spectrum are clearly resolved at rare-earth concentrations $\leq 0.1\%$. Also, optical hole burning in this site[2] takes place via a mechanism involving the coupling between the rare-earth ion and the surrounding fluorine spins. This provides a method for optical detection of near-neighbor fluorine nuclear magnetic resonance (ODNMR), which was used to determine the magnitudes and directions of the Pr^{3+} magnetic field at the local sites of the nearest-neighbor (NN) and next-nearest-neighbor (NNN) fluorines.

Since there are virtually no covalent-bonding effects between the Pr^{3+} ion and its next-nearest neighbors, the positions of these fluorines were determined from the measured local Pr^{3+} fields.

The substitution of a Pr^{3+} for a Ca^{2+} ion and the insertion of an interstitial fluorine was found to have distorted the lattice in such a way that the NNN fluorines were all pushed away from the Pr^{3+}, and toward each other, except for the four NNN's furthest from the interstitial, whose positions were not shifted. Strong covalent-bonding effects prevented a similar determination of the nearest-neighbor (NN) and interstitial (*i*) fluorine positions, but the local-field *directions* indicate that the covalent bonding is nearly point dipolar in form.

A model based on near-neighbor fluorine spin flips while the Pr^{3+} ion is in its ground state agrees well with the observed optical hole width. Furthermore, an explanation of these spin flips as due primarily to ground-state Pr^{3+} electron transitions coupled with either an applied external field or the local field due to other fluorines, is supported qualitatively by the observed dependence of the ODNMR line strength on the applied field and the orientation of the C_4 axis. The observation of rf-assisted hole burning at 16.6 kG with $C_4 \| \vec{H}_0$ further supports this picture.

ACKNOWLEDGMENTS

The authors wish to thank Don Horne for the design and construction of the traveling-wave rf coil used in these experiments. This work was supported in part by the U. S. Air Force Office of Scientific Research (AFSC) under Contract No. F 49620-79-C-0108.

[1]L. Q. Lambert, Phys. Rev. B 7, 1834 (1973); R. M. Macfarlane, R. M. Shelby, and R. L. Shoemaker, Phys. Rev. Lett. 43, 1726 (1979); S. C. Rand, A. Wokaun, R. G. DeVoe, and R. G. Brewer, Phys. Rev. Lett. 43, 1868 (1979); R. M. Macfarlane, C. S. Yannoni, and R. M. Shelby, Opt. Commun. 32, 101 (1980).

[2]R. M. Macfarlane, R. M. Shelby, and D. P. Burum, Opt. Lett. 6, 593 (1981).

[3]W. B. Mims, in *Electron Paramagnetic Resonance,* edited by S. Geschwind (Plenum, New York, 1972), p. 263; A. D. A. Hansen and J. P. Wolfe, Phys. Lett. 66A, 320 (1978); R. M. Shelby, C. S. Yannoni, and R. M. Macfarlane, Phys. Rev. Lett. 41, 1739 (1978); R. G. DeVoe, A. Wokaun, S. C. Rand, and R. G. Brewer, Phys. Rev. B 23, 3125 (1981).

[4]P. Evesque, J. Kliava, and J. Duran, J. Lumin. 18/19, 646 (1979).

[5]L. E. Erickson, Opt. Commun. 21, 147 (1977).

[6]J. P. Wolfe and R. S. Markiewicz, Phys. Rev. Lett. 30, 1105 (1973).

[7]R. W. G. Wyckoff, *Crystal Structures,* 2nd ed. (Interscience, New York, 1965), Vol. 1, p. 239.

[8]J. M. Baker, E. R. Davies, and J. P. Hurrell, Proc. Roy. Soc. London Ser. A 308, 403 (1968).

[9]G. C. Wetzel Jr., C. G. Roberts, E. L. Kitts Jr., and P. O'Hagan, Phys. Lett. 30A, 35 (1969).

[10]I. J. Lowe and M. Engelsberg, Rev. Sci. Instrum. 45, 631 (1974).

[11]P. L. Scott and C. D. Jeffries, Phys. Rev. 127, 31 (1962).